

ISS: IMAGE AS STEPPING STONE FOR TEXT-GUIDED 3D SHAPE GENERATION

Zhengzhe Liu¹ Peng Dai² Ruihui Li³ Xiaojuan Qi^{2*} Chi-Wing Fu^{1*}

¹The Chinese University of Hong Kong ²The University of Hong Kong ³Hunan University

ABSTRACT

Text-guided 3D shape generation remains challenging due to the absence of large paired text-shape data, the substantial semantic gap between these two modalities, and the structural complexity of 3D shapes. This paper presents a new framework called *Image as Stepping Stone* (ISS) for the task by introducing 2D image as a stepping stone to connect the two modalities and to eliminate the need for paired text-shape data. Our key contribution is a *two-stage feature-space-alignment approach* that maps CLIP features to shapes by harnessing a pre-trained single-view reconstruction (SVR) model with multi-view supervisions: first map the CLIP image feature to the detail-rich shape space in the SVR model, then map the CLIP text feature to the shape space and optimize the mapping by encouraging CLIP consistency between the input text and the rendered images. Further, we formulate a *text-guided shape stylization module* to dress up the output shapes with novel textures. Beyond existing works on 3D shape generation from text, our new approach is general for creating shapes in a broad range of categories, *without* requiring paired text-shape data. Experimental results manifest that our approach outperforms the state-of-the-arts and our baselines in terms of *fidelity* and *consistency with text*. Further, our approach can stylize the generated shapes with both realistic and fantasy structures and textures.

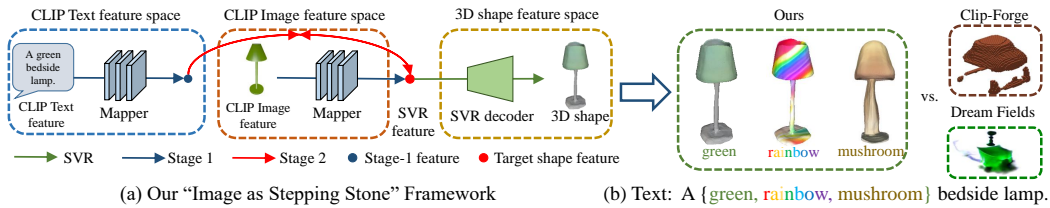


Figure 1: Our novel "Image as Stepping Stone" framework (a) is able to connect the text space (the CLIP Text feature) and the 3D shape space (the SVR feature) through our two-stage feature-space alignment, such that we can generate plausible 3D shapes from text (b) beyond the capabilities of the existing works (CLIP-Forge and Dream Fields), without requiring paired text-shape data.

1 INTRODUCTION

3D shape generation has a broad range of applications, *e.g.*, in Metaverse, CAD, games, animations, etc. Among various ways to generate 3D shapes, a user-friendly approach is to generate shapes from natural language or text descriptions. By this means, users can readily create shapes, *e.g.*, to add/modify objects in VR/AR worlds, to design shapes for 3D printing, etc. Yet, generating shapes from texts is very challenging, due to the lack of large-scale paired text-shape data, the large semantic gap between the text and shape modalities, and the structural complexity of 3D shapes.

Existing works Chen et al. (2018); Jahan et al. (2021); Liu et al. (2022) typically rely on paired text-shape data for model training. Yet, collecting 3D shapes is already very challenging on its own, let alone the tedious manual annotations needed to construct the text-shape pairs. To our best knowledge, the largest existing paired text-shape dataset Chen et al. (2018) contains only two categories, *i.e.*, table and chair, thus severely limiting the applicability of the existing works.

*: Corresponding authors.

Very recently, two annotation-free approaches, CLIP-Forge Sanghi et al. (2022) and Dream Fields Jain et al. (2022), were proposed to address the dataset limitation. These two state-of-the-art approaches attempt to utilize the joint text-image embedding from the large-scale pre-trained language vision model, *i.e.*, CLIP Radford et al. (2021), to eliminate the need of requiring paired text-shape data in model training. However, it is still extremely challenging to generate 3D shapes from text without paired texts and shapes for the following reasons. First, the range of object categories that can be generated are still limited due to the scarcity of 3D datasets. For example, Clip-Forge Sanghi et al. (2022) is built upon a shape auto-encoder; it can hardly generate plausible shapes beyond the ShapeNet categories. Also, it is challenging to learn 3D prior of the desired shape from texts. For instance, Dream Field Jain et al. (2022) cannot generate 3D shapes like our approach due to the lack of 3D prior, as it is trained to produce only multi-view images with a neural radiance field. Further, with over an hour of optimization for each shape instance from scratch, there is still no guarantee that the multi-view consistency constraint of Dream Field Jain et al. (2022) can enforce the model for producing shapes that match the given text; we will provide further investigation in our experiments. Last, the visual quality of the generated shapes are far from satisfactory due to the substantial semantic gap between the unpaired texts and shapes. As shown in Figure 1 (b), the results generated by Dream Field typically look surrealistic (rather than real), due to insufficient information extracted from text for the shape structures and details. On the other hand, CLIP-Forge Sanghi et al. (2022) is highly restricted by the limited 64^3 resolution and it lacks colors and textures, further manifesting the difficulty of generating 3D shapes from unpaired text-shape data.

Going beyond the existing works, we propose a new approach to 3D shape generation from text without needing paired text-shape data. Our key idea is to *implicitly leverage 2D image* as a stepping stone (ISS) to connect the text and shape modalities. Specifically, we employ the joint text-image embedding in CLIP and train a CLIP2Shape mapper to *map the CLIP image features to a pre-trained detail-rich 3D shape space with multi-view supervisions*; see Figure 1 (a): stage 1. Thanks to the joint text-image embedding from CLIP, our trained mapper is able to connect the CLIP text features with the shape space for text-guided 3D shape generation. Yet, due to the gap between the CLIP text and CLIP image features, the mapped text feature may not align well with the destination shape feature; see the empirical analysis in Section 3.2. Hence, we further fine-tune the mapper specific to each text input by *encouraging CLIP consistency* between the rendered images and the input text to enhance the consistency between the input text and the generated shape; see Figure 1 (a): stage 2.

Our new approach advances the frontier of 3D shape generation from text in the following aspects. First, by taking image as a stepping stone, we make the challenging text-guided 3D shape generation task more approachable and cast it as a single-view reconstruction (SVR) task. Having said that, we learn 3D shape priors from the adopted SVR model directly in the feature space. Second, benefiting from the learned 3D priors from the SVR model and the joint text-image embeddings, our approach can produce 3D shapes in only 85 seconds vs. 72 minutes of Dream Fields Jain et al. (2022). More importantly, our approach is able to produce plausible 3D shapes, *not* multi-view images, beyond the generation capabilities of the state-of-the-art approaches; see Figure 1 (b).

With our two-stage feature-space alignment, we already can generate shapes with good fidelity from texts. To further enrich the generated shapes with vivid textures and structures beyond the generative space of the pre-trained SVR model, we additionally design a text-guided stylization module to generate novel textures and shapes by encouraging consistency between the rendered images and the text description of the target style. We then can effectively fuse with the two-stage feature-space alignment to enable the generation of both realistic and fantasy textures and also shapes beyond the training data; see Figure 1 (b) for examples. Furthermore, our approach is compatible with different SVR models Niemeyer et al. (2020); Alwala et al. (2022). For example, we can adopt SS3D Alwala et al. (2022) to generate shapes from single-view in-the-wild images to broaden the range of categorical 3D shapes that our approach can generate, going beyond Sanghi et al. (2022), which can only generate 13 categories of ShapeNet; see our results in Section E. **We will release our code and trained models on GitHub after the publication of this work.**

2 RELATED WORKS

Text-guided image generation Existing text-guided image generation approaches can be roughly cast into two branches: (i) direct image synthesis Reed et al. (2016a;b); Zhang et al. (2017; 2018); Xu et al. (2018); Li et al. (2019; 2020); Qiao et al. (2019); Wang et al. (2021) and (ii) image generation

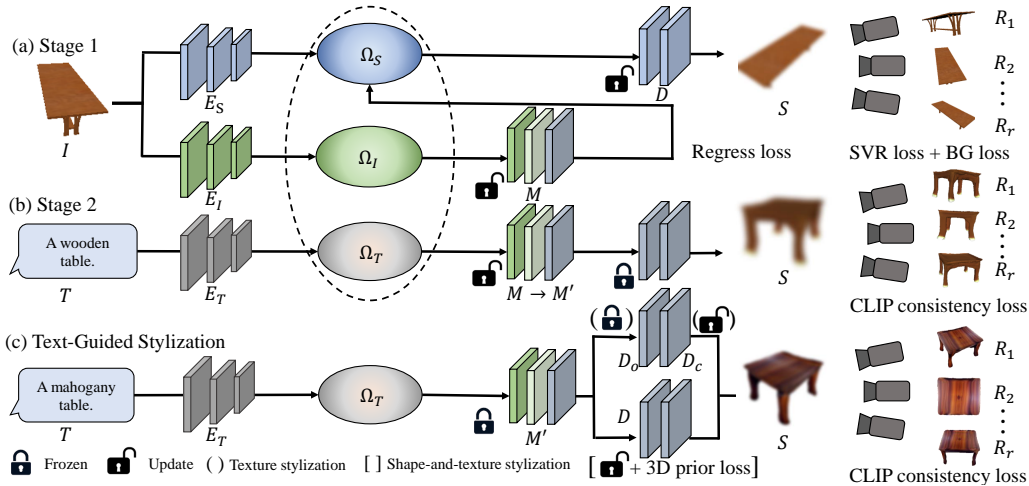


Figure 2: Overview of our text-guided 3D shape generation framework, which has three major stages. (a) Leveraging a pre-trained SVR model, in stage-1 feature-space alignment, we train the CLIP2Shape mapper M to map the CLIP image feature space Ω_I to shape space Ω_S of the SVR model, and fine-tune decoder D with an additional background loss L_{bg} . (b) In stage-2 feature-space alignment, we fix D and fine-tune M into M' by encouraging CLIP consistency between input text T and the rendered images at test time. (c) Last, we optimize the style of the generated shape and texture of S for T . At the inference, we use stage 2 to generate 3D shape from T and (c) is optional.

with a pre-trained GAN Stap et al. (2020); Yuan & Peng (2019); Souza et al. (2020); Wang et al. (2020); Rombach et al. (2020); Patashnik et al. (2021); Xia et al. (2021). Yet, the above works can only generate images for limited categories. To address this issue, some recent works explore zero-shot text-guided image generation Ramesh et al. (2021); Ding et al. (2021); Nichol et al. (2021); Liu et al. (2021); Ramesh et al. (2022) to learn to produce images of any category. Recently, Zhou et al. (2022) and Wang et al. (2022b) leverage CLIP for text-free text-to-image generation.

Text-guided shape generation is more challenging compared with text-to-image generation. First, it is far more labor-intensive and difficult to prepare a large amount of paired text-shape data than paired text-image data, which can be collected from the Internet on a large scale. Second, the text-to-shape task requires one to predict full 3D structures that should be plausible geometrically and consistently in all views, beyond the needs in single-view image generation. Third, 3D shapes may exhibit more complex spatial structures and topology, beyond regular grid-based 2D images.

Text-guided 3D generation To generate shapes from text, several works Chen et al. (2018); Jahan et al. (2021); Liu et al. (2022) rely on paired text-shape data for training. To avoid paired text-shape data, two very recent works, CLIP-Forge Sanghi et al. (2022) and Dream Fields Jain et al. (2022), attempt to leverage the large-scale pre-trained vision-language model CLIP. Yet, they still suffer from various limitations, as discussed in the third paragraph of Section 1. Besides 3D shape generation, some recent works utilize CLIP to manipulate a shape or NeRF with text Michel et al. (2022); Jetchev (2021); Wang et al. (2022a) and to generate 3D avatars Hong et al. (2022).

In this work, we present a new framework for generating 3D shape from text without paired text-shape data by our novel two-stage feature-space alignment. Our experimental results demonstrate the superiority of this work beyond the existing ones in terms of fidelity and text-shape consistency.

Single-view reconstruction Another topic related to this work is single-view reconstruction (SVR). Recently, researchers have explored SVR with meshes Agarwal & Gopi (2020), voxels Zubić & Liò (2021), and 3D shapes Niemeyer et al. (2020). Further, to extend SVR to in-the-wild categories, Alwala et al. (2022) propose SS3D to learn 3D shape reconstruction using single-view images in hundreds of categories. In our work, we propose to harness an SVR model to map images to shapes, such that we can take 2D image as a stepping stone for producing shapes from texts. Yet, we perform the mapping and feature alignment implicitly in the latent space rather than explicitly.

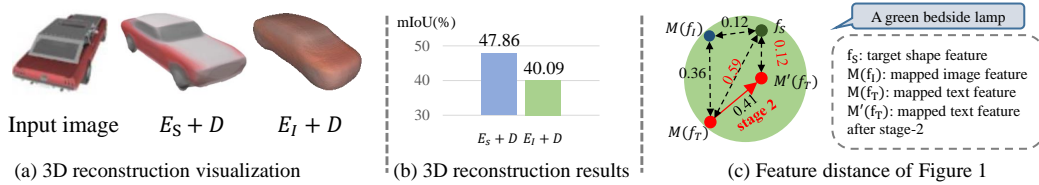


Figure 3: Empirical studies on the CLIP feature space for text-guided 3D shape generation.

3 METHODOLOGY

3.1 OVERVIEW

This work aims to generate 3D shape S from text T . Overall, our idea is to map the CLIP features to the shape space of a pre-trained SVR model, such that we can leverage the joint text-image embeddings from CLIP and also the 3D generation capability of the SVR model to enhance the generation of 3D shape from text. Hence, our method only needs to be trained with multi-view RGBD images and the associated camera poses without paired text-shape data. As Figure 2 shows, our framework includes (i) image encoder E_S , which maps input image I to SVR shape space Ω_S , (ii) pre-trained CLIP text and image encoders E_T and E_I , which map text T and image I to CLIP spaces Ω_T and Ω_I , respectively, (iii) mapper M with 12 fully-connected layers, each followed by a Leaky-ReLU, and (iv) decoder D to generate the final shape S . Specifically, we use DVR Niemeyer et al. (2020) as the SVR model when presenting our method, unless otherwise specified.

Overall, we introduce a novel two-stage feature-space-alignment approach to connect the text, image, and shape modalities. In detail, we first train CLIP2Shape mapper M to connect the CLIP image space Ω_I and the shape space Ω_S from the pre-trained SVR model (see Figure 2 (a)). Then, we fine-tune M at test time using a CLIP consistency loss L_c to further connect the CLIP text space Ω_T with Ω_S (see Figure 2 (b)). Last, we may further optimize the texture and structure style of S by fine-tuning the decoders (see Figure 2 (c)).

In the following, we first introduce two empirical studies on the CLIP feature space in Section 3.2, then present our two-stage feature-space-alignment approach in Section 3.3. Further, Section D presents our text-guided shape stylization method and Section 3.5 discusses the compatibility of our approach with different SVR models and our extension to generate a broad range of categories.

3.2 EMPIRICAL STUDIES AND MOTIVATIONS

Existing works Sanghi et al. (2022); Zhou et al. (2022); Wang et al. (2022b;a) mostly utilize CLIP directly without analyzing how it works and discussing its limitations. To start, we investigate the merits and drawbacks of leveraging CLIP for text-guided 3D shape generation by conducting the following two empirical studies to gain more insight into the CLIP feature space.

3.2.1 WHETHER CLIP FEATURE SPACE SUFFICIENTLY GOOD FOR 3D SHAPE GENERATION?

First, we study the representative capability of the CLIP image feature space Ω_I by trying to generate 3D shapes from this space. Specifically, we replace the SVR image encoder E_S with the CLIP image encoder E_I , and optimize implicit decoder D using multi-view losses like DVR Niemeyer et al. (2020) with E_I frozen. This approach can be extended to text-to-shape generation by replacing E_I with CLIP text encoder E_T during the inference. To compare the performance of E_S and E_I , we evaluate 3D mIoU between their generated shapes and GTs. The results are as follows: the standard SVR pipeline E_S+D achieves 47.86% mIoU while replacing the SVR encoder E_S with CLIP encoder E_I (E_I+D) degrades the performance to 40.09%. From the results and qualitative comparison shown in Figures 3 (a, b), we can see that the CLIP image space Ω_I has *inferior representative capability to capture details of the input image* for 3D shape generation. This is not surprising, since the pre-trained E_I from CLIP is targeted to extract semantic-aligned features from texts rather than extracting details from images. Hence, image details relevant to 3D reconstruction are lost, e.g., textures. On the contrary, E_S from the SVR model is optimized for 3D generation from images, so it maintains more necessary details. The above result motivates us to design a mapper M from Ω_I to Ω_S and then generate shapes from Ω_S instead of Ω_I for better generative fidelity.

3.2.2 HOW THE CLIP IMAGE AND TEXT FEATURE GAP INFLUENCES 3D SHAPE GENERATION?

Second, we investigate the gap between the normalized CLIP image feature $f_I \in \Omega_I$ and normalized CLIP text feature $f_T \in \Omega_T$; (see also the CLIP image and text feature spaces in Figure 1 (a)) and how such gap influences text-guided 3D shape generation. Specifically, we randomly sample 300 text-shape pairs from the text-shape dataset Chen et al. (2018), then evaluate the cosine distance between f_I and f_T , *i.e.*, $d = 1 - \text{cosine_similarity}(f_I, f_T)$, where f_I is the CLIP feature of the rendered images from the corresponding shape. We repeat the experiment and obtain $d(f_T, f_I) = 0.783 \pm 0.004$. The result reveals *a certain gap between the CLIP text and image features in this dataset, even though they are paired*. Also, the angle in the feature space between the two features is around $\arccos(1 - 0.783) = 1.35$ rad in this dataset Chen et al. (2018). Having said that, directly replacing f_I with f_T like Sanghi et al. (2022); Zhou et al. (2022) in inference may harm the consistency between the output shape and the input text. Taking Figure 1 as an example, directly replacing f_I with f_T causes 0.59 cosine distance to $f_S \in \Omega_S$ (see Figure 3 (c)), which is significantly larger than the distance between f_I and f_S (0.12). This finding motivates us to further fine-tune M into M' at test time, such that we can produce feature $M'(f_T)$, which is closer to f_S than $M(f_T)$.

3.3 TWO-STAGE FEATURE-SPACE ALIGNMENT

Following the above findings, we propose a two-stage feature-space-alignment approach to first connect image space Ω_I and shape space Ω_S and further connect text space Ω_T to shape space Ω_S with the image space Ω_I as the stepping stone.

Stage-1 alignment: CLIP image-to-shape mapping Given multi-view RGBD images for training, the stage-1 alignment is illustrated in Figure 2 (a). Considering that shape space Ω_S contains richer object details than the image space Ω_I , while Ω_I provides a joint text-image embedding with input text space Ω_T , we introduce a fully-connected CLIP2Shape mapper M to map image feature f_I to shape space Ω_S . Taking a rendered image I as input, M is optimized with an L_2 regression between $M(f_I)$ and standard SVR feature $f_S = E_S(I)$ according to Equation 1 below:

$$L_M = \sum_{i=1}^N \|M(f_{I,i}) - E_S(I_i)\|_2^2 \quad (1)$$

where N is the number of images in the training set and $f_{I,i}$ is the normalized CLIP feature of I_i .

Also, we fine-tune decoder D to encourage it to predict a white background, which helps the model to ignore the background and extract object-centric feature (see Figure 4), while maintaining its 3D shape generation capability. To this end, we propose a new background loss L_{bg} in Equation 2 below to enhance the model’s foreground object awareness to prepare for the second-stage alignment.

$$L_{bg} = \sum_p \|D_c(p) - 1\|_2^2 \mathbb{1}(\text{ray}(o, p) \cap F = \emptyset) \quad (2)$$

where $\mathbb{1}$ is the indicator function; $F = \{p : D_o(p) > t\}$ indicates the foreground region, in which the occupancy prediction $D_o(p)$ is larger than threshold t ; p is a query point; $\text{ray}(o, p) \cap F = \emptyset$ means the ray from camera center o through p does not intersect the foreground object marked by F ; and $D_c(p)$ is the color prediction at query point p . In a word, L_{bg} encourages D to predict the background region as white color (value 1), such that E_I can focus on and better capture the foreground object. In addition, to preserve the 3D shape generation capability of D , we follow the loss L_D , with which D has been optimized in the SVR training. In this work, we adopt Niemeyer et al. (2020).

Hence, the overall loss in stage-1 training is $\lambda_M L_M + \lambda_{bg} L_{bg} + L_D$, where λ_M and λ_{bg} are weights. The stage-1 alignment provides a good initialization for the test-time optimization of stage 2.

Stage-2 alignment: text-to-shape optimization Given a piece of text, the stage-2 alignment aims to further connect the text and shape modalities. Specifically, it searches for shape S that best matches the input text T . To this end, we formulate a fast test-time optimization to reduce the gap between the text and image CLIP features f_T and f_I , as discussed earlier in the second empirical study.

As shown in Figure 2 (b), given input text T , we replace image encoder E_I with text encoder E_T to extract CLIP text feature f_T , then fine-tune M with CLIP consistency loss between input text T and

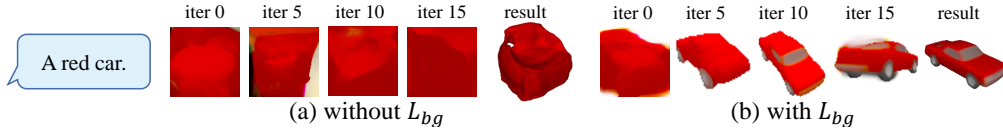


Figure 4: Effect of generating shapes from the same text with/without background loss L_{bg} .

m images $\{R_i\}_{i=1}^m$ rendered with random camera poses from output shape S ; see Equation 3:

$$L_C = \sum_{i=1}^m \langle f_T \cdot \frac{E_1(R_i)}{\|E_1(R_i)\|} \rangle \quad (3)$$

where $\langle \cdot \rangle$ indicates the inner-product.

In stage-2 alignment, we still adopt L_{bg} to enhance the model’s foreground awareness. Comparing Figures 4 (a) and (b), we can see that the stage-2 alignment is able to find a rough shape with L_{bg} in around five iterations, yet failing to produce a reasonable output without L_{bg} , since having the same color prediction on both foreground and background hinders the object awareness of the model.

Thanks to the joint text-image embedding of CLIP, the gap between text feature f_T and shape feature f_S has already been largely narrowed by M . Therefore, the stage-2 alignment only needs to fine-tune M with 20 iterations using the input text, taking only around 85 seconds on a single GeForce RTX 3090 Ti, compared with 72 minutes taken by Dream Fields Jain et al. (2022) at test time. After this fine-tuning, we can readily obtain a plausible result; see, *e.g.*, the “result” shown in Figure 4 (b). Our ISS is a novel and efficient approach for 3D shape generation from text.

Diversified generation In general, shape generation from text is one-to-many. Hence, we further extend our approach with diversified 3D shape generation from the same piece of input text. Unlike the existing works, which require additional and complex modules, *e.g.*, GANs Chen et al. (2018), IMLE Liu et al. (2022), and normalizing flow network Sanghi et al. (2022), we can simply perturb the image and text features for diversified generation. Specifically, after stage-1 alignment, we randomly permute f_I as an initialization and f_T as the ground truth by adding normalized Gaussian noises $z_1 = h_1/\|h_1\|$, $z_2 = h_2/\|h_2\|$, where $h_1, h_2 \sim N(0, 1)$ to derive diversified features

$$\hat{f}_I = \tau_1 f_I + (1 - \tau_1) z_1 \quad \text{and} \quad \hat{f}_T = \tau_2 f_T + (1 - \tau_2) z_2, \quad (4)$$

where τ_1, τ_2 are hyperparameters to control the degrees of permutation. With permuted \hat{f}_I and \hat{f}_T in stage-2 alignment, our model can converge to different 3D shapes for different noise.

3.4 TEXT-GUIDED STYLIZATION

The two-stage feature-space alignment is already able to generate plausible 3D shapes; see, *e.g.*, Figures 2 (b) and 4 (b). However, the generative space is limited by the representation capability of the employed SVR model, *e.g.*, DVR Niemeyer et al. (2020) can only generate shapes with limited synthetic patterns as those in ShapeNet. However, a richer and wider range of structures and textures are highly desired. To this end, we propose a text-guided stylization approach to enhance the generated shapes with novel structure and texture appearances, as shown in Figures 2 (c) and 1.

Specifically, for texture stylization, we first duplicate D (except for the output layer) to be D_o and D_c , then put the output occupancy prediction layer and color prediction layer on top of D_o and D_c , respectively. Further, we fine-tune D_c with the same CLIP consistency loss as in Equation 3, encouraging the consistency between input text T and the m rendered images $\{R_i\}_{i=1}^m$.

Besides textures, novel structures are also desirable for the shape stylization. Therefore, we further propose a shape-and-texture stylization strategy to create novel structures. To enable shape sculpting, we fine-tune D with the same CLIP consistency loss in Equation 3. At the same time, to maintain the overall structure of the initial shape S , we propose a 3D prior loss L_P shown in Equation 5, aiming at preserving the 3D shape prior learned by the two-stage feature-space alignment.

$$L_P = \sum_p |D_o(p) - D'_o(p)| \quad (5)$$

where p is the query point, and D_o, D'_o are the occupancy predictions of the initial D and the fine-tuned D in the stylization process, respectively. To improve the consistency between the generated texture and the generated shape, we augment the background color of R_i with a random RGB value in each iteration. Please find more details in the supplementary material.

3.5 COMPATIBILITY WITH DIFFERENT SVR MODELS

Besides DVR Niemeyer et al. (2020), our ISS framework is compatible with different SVR models. For example, we can adapt it with the most recent SVR approach SS3D Alwala et al. (2022) that leverages in-the-wild single images for 3D generation. With this model, our framework can generate a wider range of shape categories by using SS3D’s encoder and decoder as shape encoder E_S and decoder D in our framework, respectively. Here, we simply follow the same pipeline as in Figure 2 to derive a text-guided shape generation model for the in-the-wild categories; see our results in Section 4.4. Notably, we follow the losses in Alwala et al. (2022) in place of L_D (see Section 3.3) in stage-1 training, requiring only single-view images without camera poses. More importantly, our approach’s high compatibility suggests that it is orthogonal to SVR, so its performance can potentially be further upgraded with more advanced SVR approaches in the future.

4 EXPERIMENTS

4.1 DATASETS, IMPLEMENTATION DETAILS, AND METRICS

With multi-view RGBD images and camera poses, we can train ISS on the synthetic dataset ShapeNet Chang et al. (2015) (13 categories) and the real-world dataset CO3D Reizenstein et al. (2021) (50 categories). To evaluate our generative performance, we create a text description set with four texts per category on ShapeNet and two texts per category on CO3D. SS3D Alwala et al. (2022) takes single-view in-the-wild images in training; as their data has not been released, we only evaluate our method on some of their categories. To evaluate the performance, we employ Fréchet Inception Distance (FID) Heusel et al. (2017), Fréchet Point Distance (FPD) Liu et al. (2022) to measure shape generation quality, and conduct a human perceptual evaluation to further assess text-shape consistency. Please refer to the supplementary material for more details on the metrics and implementation details.

4.2 COMPARISONS WITH STATE-OF-THE-ART METHODS

We compare our approach with existing works Sanghi et al. (2022); Jain et al. (2022), both qualitatively and quantitatively. For a fair comparison, we use their official codes on GitHub to generate shapes on our text set. Table 1 shows the quantitative comparisons, whereas Figure 5 shows the qualitative comparisons. Comparing the “Existing works” and “Ours” sections in Table 1 (and also Figure 5 (a,b,i)), we can see that our approach outperforms the two state-of-the-art works by a large margin for both generative quality and text-shape consistency scores. On the other hand, the qualitative comparisons in Figure 5 (a,b) demonstrate that CLIP-Forge Sanghi et al. (2022) produces low-resolution shapes without texture and some generative shapes are inconsistent with the input text, *e.g.*, “a wooden boat.” Dream Fields Jain et al. (2022) cannot generate reasonable shapes from the input text on the top row and its generated shape on the bottom row is also inconsistent with the associated input text. On the contrary, our approach (Figure 5 (i)) can generate high-fidelity shapes that better match the input text. Note that we only utilize two-stage feature-space alignment without stylization in producing our results. Please refer to the supplementary file for more results and visual comparisons.

4.3 ABLATION STUDIES

To manifest the effectiveness of our approach, we conduct ablation studies on the following baselines (see Table 1 and Figure 5): generate shapes from $\Omega_I (E_I + D)$, optimize stage-2 alignment without stage-1 (w/o stage 1), conduct stage-1 alignment without stage-2 (w/o stage 2), disable the background loss (w/o L_{bg}), and two additional baselines that first create images and then 3D shapes (GLIDE+DVR, LAFITE+DVR). More details on the setup and analysis are provided in the supplementary material.

4.4 MORE ANALYSIS ON GENERATIVE RESULTS OF ISS

Next, we present evaluations on the generative novelty and diversity, as well as the scalability of our two-stage feature-space alignment. Then, we show more text-guided stylization results and how our ISS approach generalizes to a wide range of categories and generates shapes with better fidelity.

Table 1: Quantitative comparisons with existing works and baselines.

Category	Method	FID (\downarrow)	Consistency Score (%) (\uparrow)	FPD (\downarrow)	A/B/C Test
Existing works	CLIP-Forge	162.87	41.83 \pm 17.62	37.43	8.90 \pm 4.12
	Dearm Fields	181.25	25.38 \pm 12.33	N.A.	N.A.
Ablation Studies	E_1+D	181.88	20.97 \pm 13.59	38.61	N.A.
	w/o Stage 1	222.96	1.92 \pm 2.22	79.41	N.A.
	w/o Stage 2	202.33	29.52 \pm 14.86	41.71	N.A.
	w/o L_{bg}	178.34	30.96 \pm 15.49	40.98	N.A.
Text2Image+SVR	GLIDE+DVR	212.41	8.85 \pm 7.94	41.33	N.A.
	LAFITE+DVR	135.01	52.12 \pm 11.05	37.55	11.70 \pm 4.11
Ours	ISS	128.68	60.0 \pm 10.94	36.03	21.70 \pm 5.19

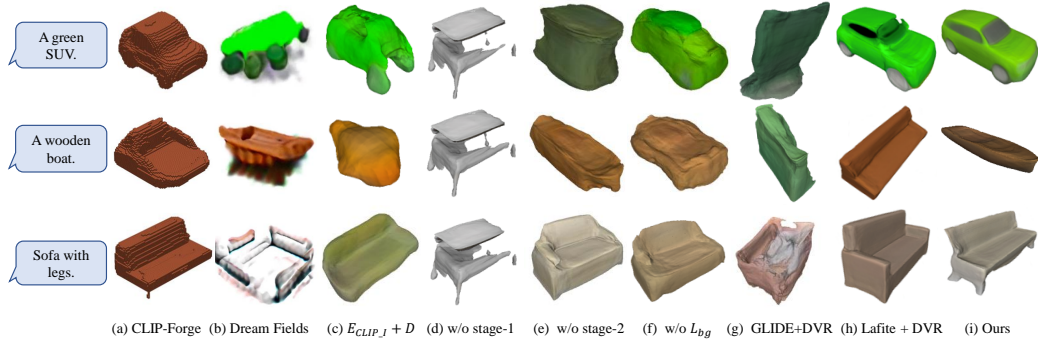


Figure 5: Qualitative comparisons with existing works and baselines.

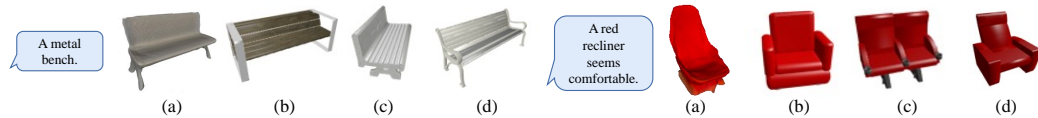


Figure 6: Our approach is able to generate novel shapes, not in the training set. (a) shows our results and (b,c,d) are the top-three shapes retrieved from the training set.



Figure 7: Our approach can generate diversified results from the same input text.

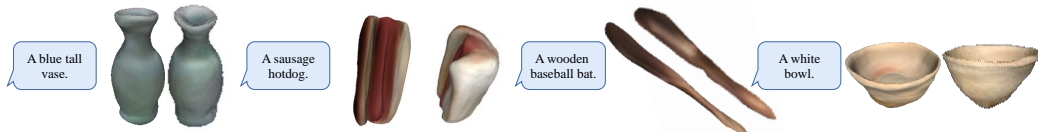


Figure 8: Results on CO3D dataset. We show two different views of each result.



Figure 9: Text-guided stylization. Left: texture stylization. Right: shape-and-texture stylization.

Novel shape generation Our approach is able to generate novel shapes beyond simple retrieval from the training data. As shown in Figure 6, from the input text, we first generate our result in (a) and then take our generated shape to retrieve the top-three closest shapes in the associated training set based on the cosine similarity between the CLIP features of the rendered images f_I and input text f_T as the retrieval metric. Our results with the two-stage feature-space alignment are not in the training sets, showing that our ISS approach can generate novel shapes beyond the training set, even without

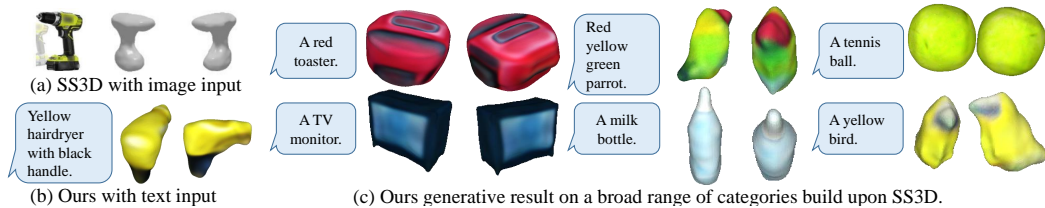


Figure 10: With single images for training (without camera poses), our approach can produce results for a broad range of categories, by adopting Alwala et al. (2022). Two different views are rendered.

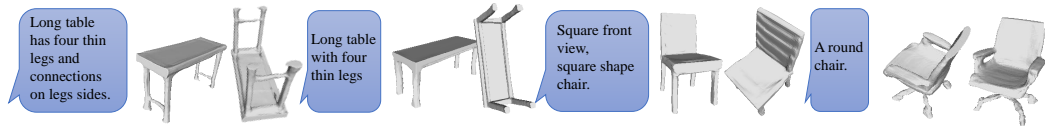


Figure 11: Results of ISS built upon the SVR model of IM-Net Chen & Zhang (2019).

stylization. It is not surprising, as our approach shares the generative space with the pre-trained SVR model and can potentially generate all shapes that the pre-trained SVR model can produce.

Diversified generation Also, our approach is able to generate diversified results from the same text input. As shown in Figure 7, ISS produces various cars and chairs from the same piece of text. Quantitative results are provided in the supplementary material.

Real-world generation on CO3D dataset To verify the scalability of ISS to real-world shapes, we present shape generation results on the real-world CO3D dataset Reizenstein et al. (2021) in Figure 8. As far as we know, this is the first work that investigates real-world text-guided 3D shape generation, so we just report that we achieve 124.31 FID on CO3D dataset, as a baseline for future works.

Text-guided stylization results beyond training set More text-guided stylization results are shown in Figure 9, in addition to Figure 1 (b) and Figure 2 (c). Our text-guided stylization approach is able to create both realistic and fantasy novel structures and textures that do not exist in the training data.

Generality of ISS to broad range of categories As shown in Figure 10, our approach can generate more categories built upon SS3D Alwala et al. (2022) beyond those in ShapeNet and CO3D, *e.g.*, birds. In training, both SS3D and ours only utilize single images of these categories without camera pose. Like Alwala et al. (2022), we utilize the ground-truth object masks of the bird category, and derive masks of the other categories with an off-the-self semantic segmentation model. As shown in Figure 10 (a,b), our approach with only text as the input can generate shapes with comparable or even better quality compared with Alwala et al. (2022) that takes an image as input. Further, going beyond Alwala et al. (2022), our novel approach can create 3D shapes with textures, thanks to our text-guided texture stylization (see Figure 10 (c)). In addition, Figure 10 (c) further manifests that our stylization module can generate textures that are well-consistent with the shape.

Generating 3D shapes with better fidelity Thanks to the compatibility of our ISS to different SVR models, the generative quality of our model can be *further enhanced* when adopting a stronger SVR model of IM-Net Chen & Zhang (2019), as shown in Figure 11.

5 CONCLUSION

In this paper, we present a novel approach for text-guided 3D shape generation by leveraging the image modality as a stepping stone. Leveraging the joint text-image embeddings from CLIP and 3D shape priors from a pre-trained SVR model, our approach eliminates the need for the paired text and shape data. Technically, we have the following contributions. First, we step-by-step reduce the semantic gap among the text, image and shape modalities through our two-stage feature-space alignment approach. Second, our text-guided stylization technique effectively enriches our generated shapes with novel structures and textures in various styles. Third, our approach is compatible with various single view reconstruction approaches and can be further extended to generate a wide range of categories with only single images without camera poses in training. Experiments on ShapeNet, CO3D, and multiple single-image categories manifest the superiority of our framework over the two state-of-the-art methods and various baselines. Limitations are discussed in the supplementary files.

Supplementary Material

In this supplementary material, we first introduce the background augmentation in text-guided shape stylization (Section A). Then, we present the implementation details and evaluation metrics, and provide the details of human perceptual evaluation results (Section B). Further, we introduce the setup and analysis of our ablation studies (Section C). Then, we discuss the text-guided stylization and provide more results (Section D). Also, we show additional generative results of our approach (Section E). Then we discuss two alternative training strategies (Section F). Last, we discuss the failure cases (Section G) and limitations of this work (Section H) and provide also our text sets (Section I).

A BACKGROUND AUGMENTATION IN TEXT-GUIDED SHAPE STYLIZATION

One important thing in text-guided shape stylization is that the generated texture should align with the given shape. However, it cannot be ensured with a simple white or black background during training since the generated textures can be affected by the background color. As shown in Figure 12 (a), the shape in white color may confuse with the white background; thus, the model would struggle to capture the boundary of the object, hence cannot generate textures that well-align with the table. In Figure 12 (c), the generated texture is severely affected by the black background color, causing low-quality stylization results.

To address the above issue, we propose a background augmentation approach to improve the texture-shape alignment. Specifically, the background color is replaced with random RGB values in each training iteration. By this means, the foreground shape may be more easily captured in training as shown in Figure 12 (b,d), improving the texture-shape consistency and the stylization quality.

Discussion on L_{bg} and background augmentation In two-stage feature space alignment (Section 3.3 in main paper), we introduce a background loss L_{bg} to encourage the color prediction on the background region to be white. A natural question is whether we can use background augmentation as a replacement, and our answer is no. As shown in Figure 13 (a), the background color can affect the cosine similarity of CLIP features between the image and input text; thus, using different background color in each iteration makes the stage-2 alignment unstable and affects shape generation. As a result, the two-stage alignment can only benefit from L_{bg} , but not from the background augmentation, for producing a plausible shape. Besides, we empirically found that the two-stage feature space alignment with L_{bg} performs well, even if a white shape is being considered, see the bottom row in Figure 14 (i).

On the other hand, shape stylization benefits from the background augmentation, since only texture is updated with the shape fixed in the stylization process, which makes stylization an easier task compared with the two-stage alignment, and can tolerate feature variations with different background colors.

B IMPLEMENTATION DETAILS, METRICS, AND HUMAN PERCEPTUAL EVALUATION DETAILS

Implementation details Our framework is implemented using PyTorch ?. We first train the stage-1 CLIP-image-to-shape mapping for 400 epochs with learning rate $1e^{-4}$, then train the stage-2 text-to-shape optimization at test time for 20 iterations, taking only 85 seconds on average on a single GeForce RTX 3090 Ti. Optionally, we can further train text-guided stylization with the same learning rate. We empirically set hyperparameters $\lambda_M, \lambda_{bg}, t, m, \tau_1, \tau_2$ to be 0.5, 10, 0.5, 10, 0.2, 0.95, respectively, according to a small validation set.

Metric: Shape generation quality To measure the shape generation quality, we employ Fréchet Inception Distance (FID) Heusel et al. (2017) between five rendered images of the generated shape with different camera poses and a set of ground-truth ShapeNet images. Further, we adopt the metric Fréchet Point Distance (FPD) proposed in Liu et al. (2022) to evaluate the generative quality using

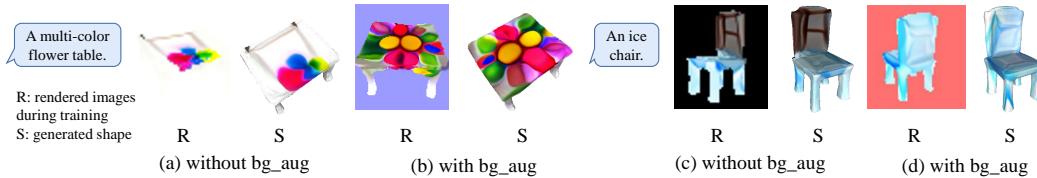


Figure 12: Effective of text-guided shape stylization with/without background augmentation.

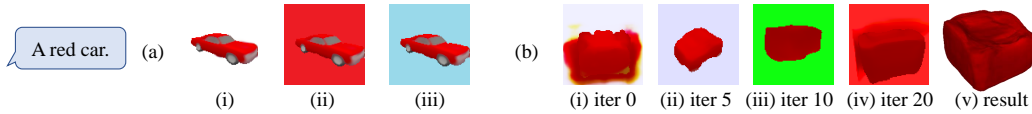


Figure 13: An investigation on background loss and background augmentation. (a) Background color affects the cosine similarity of the CLIP features between the image and the text “a red car”, *i.e.*, (i) 0.292 (ii) 0.303 and (iii) 0.285. (b) Effect of generating shapes with background augmentation, but without background loss L_{bg} . Comparing with Figure 4 (b) in the main paper, the two-stage feature space alignment works well with L_{bg} , but fails with the background augmentation.

3D point clouds. Note that Dream Field Jain et al. (2022) does not produce 3D shapes directly, so is not applicable to evaluate this work. To further assess the text-shape consistency, we conduct a human perceptual evaluation.

Metric: Human perceptual evaluation Setup We recruited 10 volunteers (three females and seven males; aged 19 to 58; all with normal vision) in this evaluation. For each input text, we produced nine results using various methods and baselines, including CLIP-Forge Sanghi et al. (2022), Dream Fields Jain et al. (2022), six baseline methods, and our full method (as shown in Figure 5 in the main paper and Figure 14 in this supplementary material); see Section 4.2 in the main paper and Section C in this supplementary material for the details of each baseline. Then, we showed these results to the participants in random order, without revealing how each result was produced. After that, they were asked to compare how the results match the input text. Specifically, they were asked to give a score of one for perfect matches, a score of 0.5 for partial matches, and zero if not match at all. Then, for each method, we can compute metric “Consistency Score” as s/n , where s is the total score and n is the number of samples.

Details of human perceptual evaluation results We show Consistency Score and the preferences in the A/B/C test from each volunteer in Tables 2 and 3. As shown in Table 2, all ten volunteers consistently gave the highest Consistency Score to our approach, and in the A/B/C test (see Table 3), all ten volunteers prefer the results from our approach more than those produced by competitor methods. The above results further manifest the superiority of ISS beyond the state of the arts Sanghi et al. (2022); Jain et al. (2022) and all the baselines.

C ABLATION STUDIES

Baseline setups We create the following baselines in our ablation study. The first four baselines aim to manifest the effectiveness of the key modules in our approach, whereas the last two adopt

Table 2: Total scores s from the ten volunteers out of 52 generated shapes.

Method	1	2	3	4	5	6	7	8	9	10	mean \pm std	Consistency Score (%) \uparrow
CLIP-Forge	21	35	34	16.5	18.5	29	21.5	4	21	17	21.75 \pm 9.16	41.83 \pm 17.62
Dearm Fields	13	17.5	7	19	6.5	22	22	9	10	6	13.2 \pm 6.41	25.38 \pm 12.33
E_1+D	14	9.5	5	18	4.5	25	15.5	4.05	4.5	9	10.91 \pm 7.06	20.97 \pm 13.59
w/o stage-1	1.5	1	0	1.5	0	3.5	2	0	0	0.5	1.00 \pm 1.15	1.92 \pm 2.22
w/o stage-2	20	14.5	8.5	23.5	7.5	27	19	8.5	4.5	20.5	15.35 \pm 7.73	29.52 \pm 14.86
w/o L_{bg}	17.5	15.5	8.5	21	8	27	26.5	9.5	5	22.5	16.1 \pm 8.06	30.96 \pm 15.49
GLIDE+DVR	5	3.5	1.5	10	2	13	6.5	0.5	1	3	4.60 \pm 4.13	8.85 \pm 7.94
LAFITE+DVR	23	33.5	31	23	27	31.5	27.5	14.5	32.5	27.5	27.10 \pm 5.75	52.12 \pm 11.05
ISS (ours)	32	37	35.5	29.5	29	37	29	17.5	32.5	33	31.20 \pm 5.69	60.00 \pm 10.94

Table 3: A/B/C Test results of the ten volunteers. The numbers in the table indicate the number of shapes from the corresponding method he/she likes most out of the three candidates. Volunteers can optionally select “pass” instead of “A/B/C” if he cannot decide which one is the best.

Category	Method	1	2	3	4	5	6	7	8	9	10	mean \pm std \uparrow
Existing works	CLIP-Forge	9	17	12	13	6	9	3	6	6	8	8.9 \pm 4.12
SOTA Text2Image+SVR	LAFITE+DVR	9	16	9	12	7	13	9	20	8	14	11.7 \pm 4.11
Ours	ISS	27	19	21	20	17	25	19	26	13	30	21.7 \pm 5.19

state-of-the-art text-to-image generation approaches to first create images then adopt DVR Niemeyer et al. (2020) to generate shapes for a fair comparison with our approach. Note that we do not adopt the most recent SVR model SS3D Alwala et al. (2022) (which aims to work with in-the-wild images), due to its inferior generative quality and lack of texture generation.

- $E_1 + D$: As the first empirical study in Section 3.2 in the main paper, E_1 is adopted to extract the image feature f_I and D is trained for 3D shape generation from f_I without the two-stage feature-space alignment.
- w/o Stage 1: Stage-2 alignment is optimized from randomly initialized M , without stage 1.
- w/o Stage 2: Generate with M after stage 1, without the test-time optimization of stage 2.
- w/o L_{bg} : Remove L_{bg} in both stage-1 and stage-2 alignment.
- GLIDE+DVR: Use the state-of-the-art zero-shot text-guided image generation approach GLIDE Nichol et al. (2021) to generate image I from T , then use DVR Niemeyer et al. (2020) to generate S from I .
- LAFITE+DVR: Train the state-of-the-art text-guided image generation approach LAFITE Zhou et al. (2022) with ShapeNet images, then generate image I from T . Further generate S from I with DVR Niemeyer et al. (2020).

Quantitative and qualitative comparisons In this section, we analyze the results of the above baselines one by one.

First, column (c) shows that the results generated from CLIP space Ω_1 have inferior fidelity in terms of the texture (top row in Figure 14) and shape structure (bottom two rows in Figure 14) due to the limited capability of E_1 to capture details of the image.

Second, column (d) of Figure 14 indicates that without stage-1 alignment, the generated shape are almost the same whatever text T is adopted as input, since M tends to map text feature f_T to almost the same feature even though stage-2 alignment is enabled. It shows that a good initialization provided by stage-1 alignment is necessary for the test-time optimization of stage 2.

Third, as shown in column (e) of Figure 14, without Stage 2, may not align well with f_S due to the semantic gap between f_I and f_T . Now, we use Figure 15 (a) to illustrate their associated results: the model in “w/o stage 2” can generate reasonable shapes from a single image (see “SVR” in Figure 15 (a)) but fails with text as input (see “stage 1” in Figure 15 (a)); further with the stage-2 optimization, a plausible phone can be generated (see “stage 2 (ours)” in Figure 15 (a)).

In addition, stage-2 alignment cannot work properly without L_{bg} (see column (f) of Figure 14) due to the lack of foreground awareness.

Further, the images created by GLIDE Nichol et al. (2021) have a large domain gap from the training data of DVR (see Figure 15 (b)), severely limiting the performance of GLIDE+DVR (see Figure 14 (g)).

In addition, some generative results of LAFITE+DVR can be coarse (first row of the main paper and the last row of Figure 14 in this supplementary material) due to the error accumulation of the isolated two steps, *i.e.*, LAFITE and DVR, and some do not match the input text due to the semantic gap between f_I and f_T (two bottom rows of Figure 5 in the main paper and the last row of Figure 14 in this supplementary material). Despite the above, subsequently generating images then shapes is still a strong baseline that is a valuable research direction in the future.

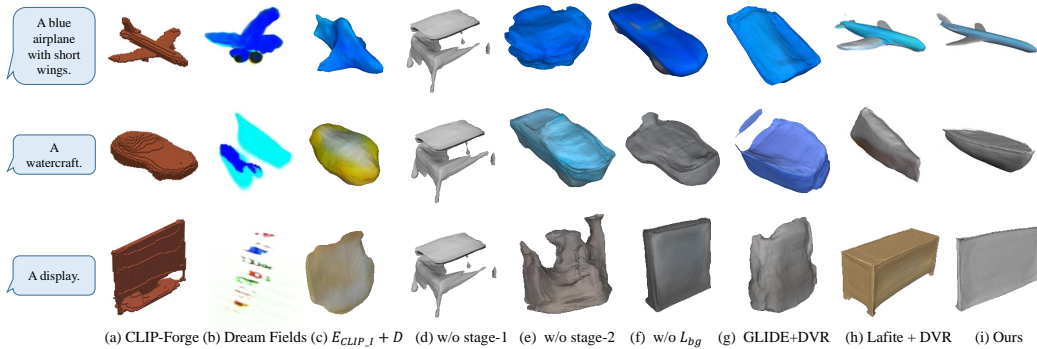


Figure 14: Additional qualitative results compared with existing works and baselines.

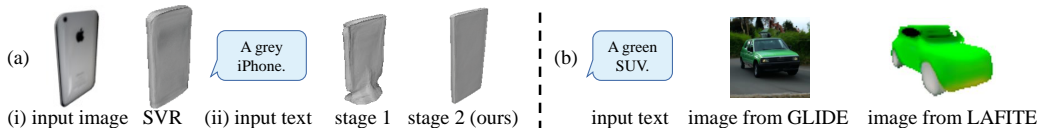


Figure 15: A further investigation on baselines “w/o stage 2”, “GLIDE+DVR”, and “LAFITE+DVR”. (a) “w/o stage 2” produces a plausible shape (“SVR”) from image but a low-quality shape (“stage 1”) from text; further fine-tuning using stage-2 alignment enables us to produce a more plausible shape from text (“stage 2 (ours)”). (b) GLIDE / LAFITE generate out-of-domain and inferior-quality images, limiting the performance of subsequent 3D generation.

Most importantly, column (i) of Figure 5 in the main paper and Figure 14 in this supplementary material shows that our approach can generate shapes and textures with good text-shape consistency (see “small wings” in the top row, “water craft” in the middle row of Figure 14) and fidelity, beyond all the above baselines and the existing works CLIP-Forge Sanghi et al. (2022) and Dream Field Jain et al. (2022).

A/B/C test To further compare our approach with the strongest baselines CLIP-Forge Sanghi et al. (2022) and “LAFITE+DVR”, we perform an A/B/C test with 10 volunteers to compare these two baselines with ours. Specifically, the results from the three approaches (per input text) in random order for all the 52 texts. Then, they were instructed to choose a most preferred one. The results in Table 1 “A/B/C Test” in the main paper show that our results are more preferred than others, outperforming Sanghi et al. (2022) by 143.8% $((21.70 - 8.90)/8.90)$ and “LAFITE+DVR” by 85.5% $((21.70 - 11.70)/11.70)$.

Diversified Generation In addition, we evaluate the diversified generation results discussed in Section 3.3 in the main paper. Specifically, we generate additional two samples per input text, and then adopt FID Heusel et al. (2017), FPD Liu et al. (2022) (the lower, the better) for the fidelity evaluation and Point Score (PS) Liu et al. (2022) (the higher, the better) for the diversity evaluation. The results are: **FID: 113.42, FPD: 33.66, PS: 3.58**, which is even better than our one-text-one-shape generative results (FID: 128.68, FPD: 36.03, PS: 3.33). It is because the ground truth datasets adopted for the above evaluations also contain diversified samples, and the diversified results in this experiment share a more similar distribution to the GT datasets. The result manifests the superior diversified generation capability of ISS.

D DISCUSSIONS ON TEXT-GUIDED SHAPE STYLIZATION

As shown in Figure 16 (a), our text-guided shape stylization is able to generate vivid landscape and flower textures on the sofa shape. Note that the sofa is generated from the text “A sofa with black backrest” (see Figure 19 top right) with totally different initial color from the stylization results. In Figure 16 (b), we show four additional texture stylization results in addition to the Figure 10 in the main paper. As shown in Figure 16 (c), our shape-and-texture stylization is able to generate novel shapes and textures beyond the dataset, and create imaginary shapes and diversified structures. Our results achieve a good balance on the stylization and the functionality. Take the “avocado chair” as an



Figure 16: Additional stylization results.

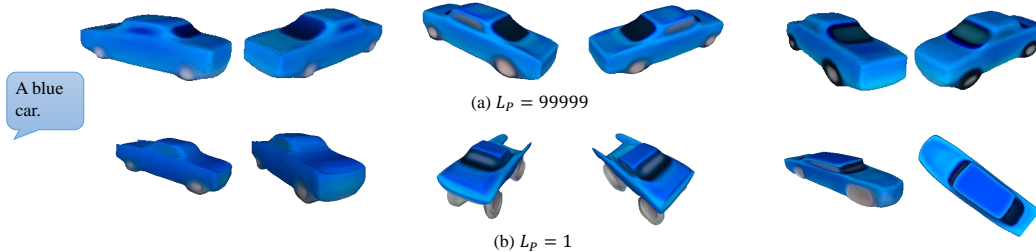


Figure 17: Results of shape-and-texture stylization with the same text “A blue car” and different 3D prior loss L_P .

example, our result better combines the style of the “avocado” and the functionality of the “chair”, compared with the result of Dream Field Jain et al. (2022), which lacks the functionality of the chair.

As shown in Figure 17, shape-and-texture stylization consistently produces the cars that is consistent with the input text “a blue car”, with proper variation in terms of the color and shape. In addition, the degree of the shape variations can be controlled by the loss weight λ_P of the 3D prior loss L_P .

Shape-and-texture stylization can produce unusual shapes In addition, our text-guided shape-and-texture stylization enables to generate unusual shapes that are out of the distribution in the training set. As shown in Figure 18, our two-stage feature-space alignment cannot generate a chair with no leg since it is significantly out of the distribution of the training set. With shape-and-texture stylization, our approach is able to generate this challenging shape. Therefore, text-guided shape-and-texture stylization enhances the generative capability of our model. Note that the texts with negative words like “no” are typically very challenging to text-guided generation approaches. For example, even the state-of-the-art text-to-image generation approach Parti ? fails to generate the cup with no juice and the plate with no banana. It further manifests the powerful generative ability of our ISS.

Why does shape-and-texture stylization need a initial shape? Shape-and-texture stylization is initialized by the two-stage feature-space alignment result, sine it provides the 3D prior.

Relationship of texture stylization and shape-and-texture stylization Texture stylization and shape-and-texture stylization have their own merits. Texture stylization keeps the shape unchanged and is able to guarantee the functionality of the shape. In addition, it can take some abstract text descriptions as input like “sunset” in Figure 16 (a). Shape-and-texture stylization is able to generate novel and imaginary structures beyond the training dataset. However, there is a tradeoff between the stylization and the functionality.

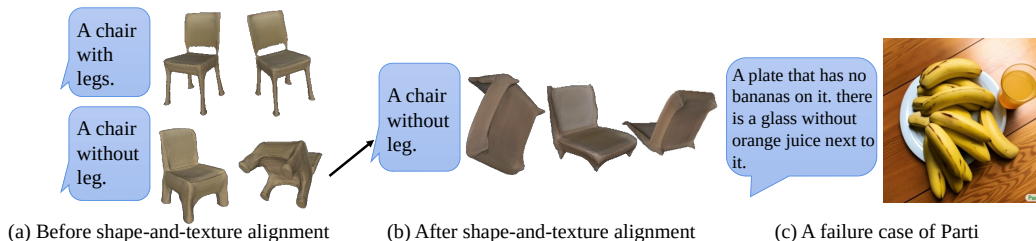


Figure 18: (a) top: results of “A chair with leg”. (a) bottom and (b): results of “A chair with no leg” before and after shape-and-texture stylization. (c). A failure case of the state-of-the-art text-to-image approach Parti ? in terms of the word “no” and “without”.

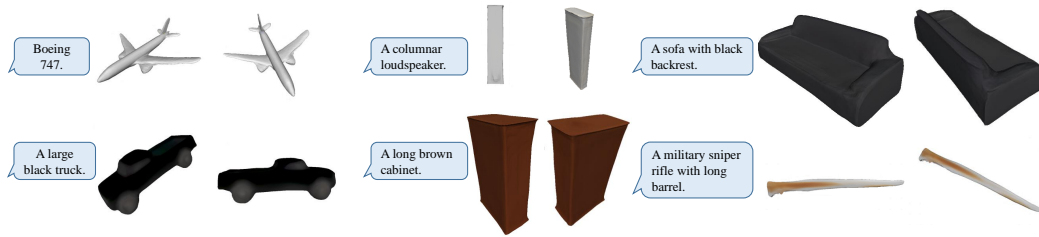


Figure 19: Additional generative results on the ShapeNet Chang et al. (2015) dataset.

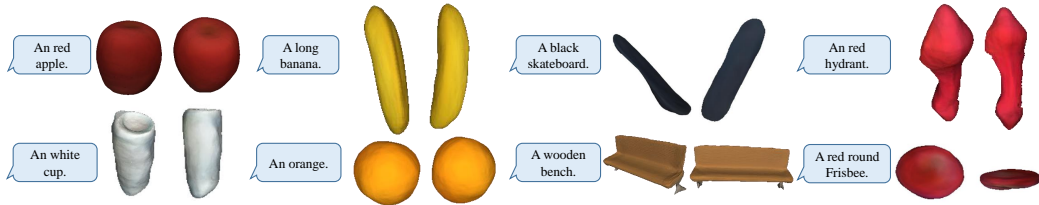


Figure 20: Additional generative results on the CO3D Reizenstein et al. (2021) dataset.

E ADDITIONAL RESULTS

ShapeNet As shown in Figure 19, our approach can generate view-consistent 3D shapes on ShapeNet Chang et al. (2015) that well match the input texts.

CO3D Further, we show more text-guided shape generation results on the CO3D Reizenstein et al. (2021) dataset in Figure 20. These results again manifest the capability of our approach on real-world 3D shape generation, beyond the existing works Chen et al. (2018); Sanghi et al. (2022); Liu et al. (2022) that focus only on the synthetic shape generation on ShapeNet Chang et al. (2015).

Single-image categories In Figure 21, we present more text-guided generations for more categories using single images in training without camera pose, built upon Alwala et al. (2022). The results further demonstrate the compatibility of our approach to various SVR approaches, particularly generating plausible 3D shapes from text with single images in training.

More generative results Further, we present more generative results of our approach in Figure 22. Using ISS, we are able to effectively generate a wide variety of 3D shapes from texts.

F DISCUSSIONS ON TWO ALTERNATIVE TRAINING STRATEGIES

Fine-tune decoder In this section, we discuss an alternative training strategy to optimize the decoder directly with the CLIP consistency loss, instead of using two-stage feature space alignment.

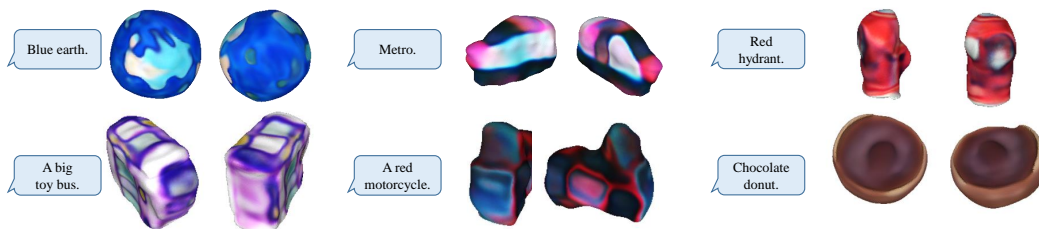


Figure 21: Additional generative results built upon SS3D Alwala et al. (2022) using single images in training without camera pose.



Figure 22: Generative results of ISS. Using our new approach, we are able to effectively produce 3D shapes for a wide variety of categories from texts.

First, we provide the results of this training strategy. It produces unsatisfactory 3D shapes such as the one shown in Figure 23 with more than 20 minutes of training. Besides, Dream Field (DF) Jain et al. (2022) also utilizes the same idea to optimize the decoder directly; yet, the generated shape (see Figure 23 (d)) is also far from satisfactory even though it is trained only to produce multi-view images with an NeRF-like architecture. Note that DF can only generate multi-view images but not 3D shapes as our method.

The pretrained decoder has already incorporated the 3D shape prior. Our approach leverages the learned shape prior and searches for the desired shape in the shape feature space Ω_S efficiently. Our approach only needs 85 seconds in the process to generate a shape.

In stage 2 (“alignment stage”), the model is trained at test time with the user-provided text. Since there is no explicit 2D/3D supervision, it is hard for the model to gain the knowledge about what the desired shape looks like. Therefore, fine-tuning the decoder in stage 2 without the explicit 2D/3D supervision will destroy the pretrained shape feature space Ω_S , which is used to introduce 3D priors. In a word, it is extremely challenging for the model to learn the 3D shape prior with only CLIP consistency supervision. Note that 3D shape generation is a very different task from shape-and-texture stylization, since shape-and-texture stylization is initialized by the two-stage feature-space alignment result, which provides the 3D prior. Therefore, we can fine-tune the decoder in shape-and-texture stylization.

Update the feature in the shape space In this section, we discuss another alternative training strategy to optimize the feature in shape space Ω_S , instead of using stage-2 feature space alignment.

First, we show the generative results of this strategy in Figure 24. In most cases, directly optimizing the 3D shape feature cannot generate satisfying results. It is because the shape feature has only 256 dimensions, which is far smaller than the number of parameters in the mapping network. Hence, it is not powerful enough to optimize the shape feature in the shape feature space.

G FAILURE CASES

Here are some examples of failure cases of our approach.

The complex and unusual shapes, e.g., “an oval table with 3 legs.” Our model fails to generate the shape from the text “an oval table with 3 legs.”. Our approach leverages the CLIP consistency loss in the rendered 2D image; however, in the rendered image shown in Figure 25 (a), only three shapes can be seen and the remaining one is occluded, which confuses the model training.

The given text is very long, e.g., “it is grey in color , circular in shape with four legs and back support, material used is wood and overall appearance looks like unique design armless chair.” Our model fails to generate the shape from the above long description as shown in Figure 25 (b). Some attributes are missing including “armless”, “four legs”. This is partially due to the limited representative capability of a single CLIP feature for such a long sentence. We may incorporate an additional local feature like Liu et al. (2022) to handle the long text in the future.

The shapes with multiple fine-grained descriptions, e.g., “A chair with a red back and a green cushion.” As shown in Figure 25 (c), our model fails to generate the shape “A chair with a red back and a green cushion.”. As studied in some recent works ??, CLIP mainly address on the global image feature, but has inferior capability to capture fine-grained features. Therefore, our approach may fail to generate shapes where multiple fine-grained descriptions are given. In the future, we may try more recent pretrained text-and-image embedding models to enhance the model’s capability to handle the fine-grained descriptions.

H LIMITATIONS

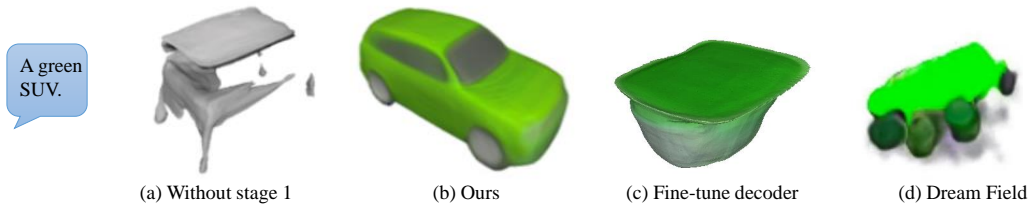


Figure 23: Results of optimizing the decoder, instead of the two-stage feature-space alignment.

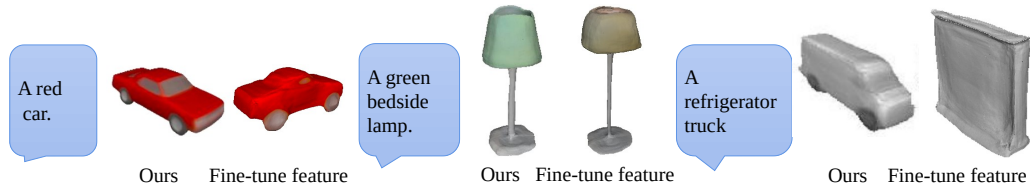


Figure 24: Results of optimizing the feature in shape space, instead of the stage 2 feature-space alignment.

This work still has some limitations. First, our performance is limited by the SVR model that our approach is built upon, *e.g.*, some results in Figure 10 of the main paper and Figure 21 in this supplementary material are still not very satisfactory, because SS3D Alwala et al. (2022) itself is struggling to create shapes with fine details. Similarly, other results built upon DVR Niemeyer et al. (2020) with unsatisfactory quality are partial due to the same reason, see Figure 26. However, at the same time, our model can benefit from stronger SVR approaches in the future to achieve better performance. An example is shown in Figure 11 where our model can generate shapes of higher quality built upon IM-Net Chen & Zhang (2019).

Second, we cannot generate the categories outside the image dataset due to the lack of 3D prior of the unseen category. That is why our model needs images as the stepping stone to learn what the particular category is like. However, we want to highlight the following. First, built upon SS3D Alwala et al. (2022), our approach can generate a wide range of categories with single view images in the wild as training data. Second, with our shape-and-texture stylization, our approach can generate imaginary and uncommon shapes outside the image dataset (in the same category). Third, it is extremely challenging to generate arbitrary category shapes from text. As far as we know, there is only one existing work, Dream Field Jain et al. (2022), that can generate more categories than ours. However, Dream field only optimizes a radiance field instead of directly generate 3D shapes, and it cannot generate reasonable shapes in many cases as shown in Figure 5 in our main paper and Figure C in this supplementary material.

I TEXT SET IN THE EXPERIMENTS

Recent works Chen et al. (2018); Sanghi et al. (2022); Jain et al. (2022) proposed their own text sets. However, their datasets have some limitations and are not suitable to evaluate our approach. The dataset of Text2shape Chen et al. (2018) contains text descriptions in only two categories, *i.e.*, Table

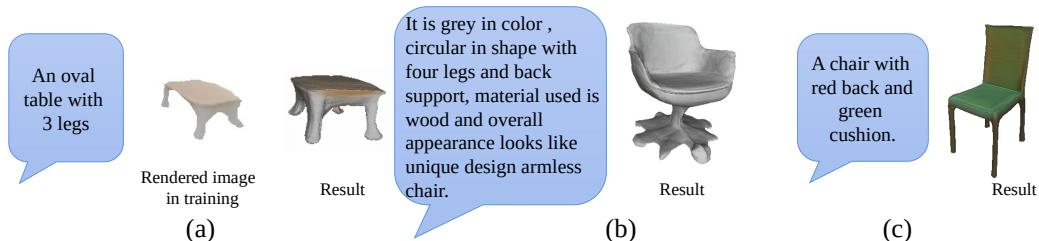


Figure 25: Failure cases of our approach.

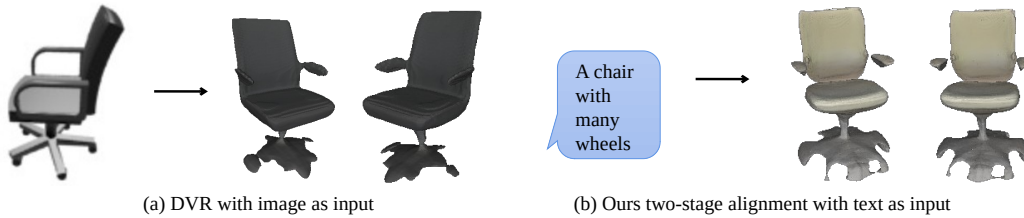


Figure 26: Our generative quality is limited by the DVR model that we build upon. (a) The result of DVR with single image as input. (b) Our result with text as input.

Table 4: Texts on ShapeNet Chang et al. (2015). They are utilized to measure FID (Table 1 of the main paper), and employed in Human Perceptual Evaluation (Table 2) and A/B/C Test (Table 3).

a glass single leg circular table	a wooden double layers table
a square metal table	a round shaped single legged wooden table
this is a bar stool with metal arches as a design feature	a children chair with little legs
a swivel chair with wheels	a red recliner seems comfortable
a red car	a green SUV
a large black truck	a long luxury black car
army fighter jet	a black airplane with long white wings
a blue airplane with short wings	boeing 747
a big ship for transportation	a boat with sail
a watercraft	a wooden boat
a blue sofa	sofa with legs
a sofa with black backrest	a small sofa
a long brown bench	a marble bench
a metal bench	concrete bench
a military sniper rifle with long barrel	a rifle with magazines
a short rifle	rifle shotgun
a computer monitor	a display
a monitor with square base	a TV monitor
a cabinet with cylindrical legs	a cupboard
a long brown cabinet	a wardrobe
a desk lamp	bedside lamp
lamp supported by a long pillar	mushroom-like lamp
a mobile phone	a small cell phone
a mobile phone with black screen	an iphone
a columnar loudspeaker	a loudspeaker with metal surface
a wooden loudspeaker	a cylindrical loudspeaker

and Chair; CLIP-Forge Sanghi et al. (2022) lacks of descriptions on the color and texture; while Dream Fields Jain et al. (2022) utilizes text descriptions containing complex scenes and actions. To fairly evaluate our approach, we propose two text datasets on the ShapeNet Chang et al. (2015) and CO3D Reizenstein et al. (2021) categories, respectively, shown in Tables 4 and 5.

REFERENCES

- Nitin Agarwal and M Gopi. Gamesh: Guided and augmented meshing for deep point networks. In *3DV*, 2020.
- Kalyan Vasudev Alwala, Abhinav Gupta, and Shubham Tulsiani. Pre-train, self-train, distill: A simple recipe for supersizing 3d reconstruction. *CVPR*, 2022.
- Angel X. Chang, Thomas Funkhouser, Leonidas J. Guibas, Pat Hanrahan, Qixing Huang, Zimo Li, Silvio Savarese, Manolis Savva, Shuran Song, Hao Su, Jianxiong Xiao, Li Yi, and Fisher Yu. ShapeNet: An Information-Rich 3D Model Repository. Technical Report arXiv:1512.03012 [cs.GR], 2015.
- Kevin Chen, Christopher B Choy, Manolis Savva, Angel X Chang, Thomas Funkhouser, and Silvio Savarese. Text2shape: Generating shapes from natural language by learning joint embeddings. In *ACCV*, 2018.

Table 5: Texts on CO3D Reizenstein et al. (2021).

A big apple	A red apple	A green bottle	A tall cylindrical bottle
A white cup	A wooden cup	A large black microwave	A white cuboid microwave
A black skateboard	A green long skateboard	A cute toytruck	A large toy truck
A blue backpack	A red big backpack	A white bowl	A big wooden bowl
A red round frisbee	A blue large frisbee	A big blue motorcycle	A black large wheels motorcycle
A circular stop sign	A triangle stop sign	Tv screen	A grey big tv screen
A basketball	A tennis ball	A large broccoli	A green broccoli
A hairdryer	A yellow hairdryer	A black mouse	A white mouse
A cuboid big suitcase	A large size tall suitcase	A round umbrella	A big black umbrella
A big banana	A long banana	A cream round cake	A chocolate mooncake
A blue handbag	A red big handbag	An orange	A large round orange
A teddybear	A cute teddybear	A blue fat vase	A blue tall vase
A black baseball bat	A long wooden baseball bat	A blue car	A red car
An egg hotdog	A sausage hotdog	A black parkingmeter	A white tall parkingmeter
A black toaster	A round toaster	Tall wineglass	Single leg big wineglass
A brown baseball glove	A black big baseball glove	A big carrot	A long carrot
A red hydrant	A yellow hydrant	A large round pizza	A tomato meat pizza
A white toilet	A fat white toilet	A stone bench	A wooden long bench
A gray iphone	A black phone	A long black keyboard	A short white keyboard
A short tree	A tall green tree	A toy bus	One decker toy bus
A blue bicycle	A black bicycle	A blue chair	A wooden chair
A red kite	A long blue kite	A TV remote	A long white remote
A book with blue cover	A black book	Brown couch	A long brown couch
A open laptop	A black laptop	An egg sandwich	A meat sandwich
A cute toy train	A short blue toy train	Chocolate donut	Big circular donut

Zhiqin Chen and Hao Zhang. Learning implicit fields for generative shape modeling. In *CVPR*, 2019.

Ming Ding, Zhuoyi Yang, Wenyi Hong, Wendi Zheng, Chang Zhou, Da Yin, Junyang Lin, Xu Zou, Zhou Shao, Hongxia Yang, et al. Cogview: Mastering text-to-image generation via transformers. *NeurIPS*, 2021.

Martin Heusel, Hubert Ramsauer, Thomas Unterthiner, Bernhard Nessler, and Sepp Hochreiter. GANs trained by a two time-scale update rule converge to a local Nash equilibrium. *NIPS*, 2017.

Fangzhou Hong, Mingyuan Zhang, Liang Pan, Zhongang Cai, Lei Yang, and Ziwei Liu. Avatarclip: Zero-shot text-driven generation and animation of 3d avatars. *arXiv preprint arXiv:2205.08535*, 2022.

Tansin Jahan, Yanran Guan, and Oliver van Kaick. Semantics-guided latent space exploration for shape generation. In *COMPUT GRAPH FORUM*, 2021.

Ajay Jain, Ben Mildenhall, Jonathan T Barron, Pieter Abbeel, and Ben Poole. Zero-shot text-guided object generation with drefam fields. In *CVPR*, 2022.

Nikolay Jetchev. ClipMatrix: Text-controlled creation of 3d textured meshes. *arXiv preprint arXiv:2109.12922*, 2021.

Bowen Li, Xiaojuan Qi, Thomas Lukasiewicz, and Philip H. S. Torr. Controllable text-to-image generation. *NeurIPS*, 2019.

Bowen Li, Xiaojuan Qi, Thomas Lukasiewicz, and Philip H. S. Torr. ManiGAN: Text-guided image manipulation. In *CVPR*, 2020.

Xingchao Liu, Chengyue Gong, Lemeng Wu, Shujian Zhang, Hao Su, and Qiang Liu. FuseDream: Training-free text-to-image generation with improved CLIP+ GAN space optimization. *arXiv preprint arXiv:2112.01573*, 2021.

Zhengzhe Liu, Yi Wang, Xiaojuan Qi, and Chi-Wing Fu. Towards implicit text-guided 3d shape generation. In *CVPR*, 2022.

Oscar Michel, Roi Bar-On, Richard Liu, Sagie Benaim, and Rana Hanocka. Text2mesh: Text-driven neural stylization for meshes. In *CVPR*, 2022.

Alex Nichol, Prafulla Dhariwal, Aditya Ramesh, Pranav Shyam, Pamela Mishkin, Bob McGrew, Ilya Sutskever, and Mark Chen. GLIDE: Towards photorealistic image generation and editing with text-guided diffusion models. *arXiv preprint arXiv:2112.10741*, 2021.

-
- Michael Niemeyer, Lars Mescheder, Michael Oechsle, and Andreas Geiger. Differentiable volumetric rendering: Learning implicit 3D representations without 3D supervision. In *CVPR*, 2020.
- Or Patashnik, Zongze Wu, Eli Shechtman, Daniel Cohen-Or, and Dani Lischinski. StyleCLIP: Text-driven manipulation of StyleGAN imagery. *ICCV*, 2021.
- Tingting Qiao, Jing Zhang, Duanqing Xu, and Dacheng Tao. MirrorGAN: Learning text-to-image generation by redescription. In *CVPR*, 2019.
- Alec Radford, Jong Wook Kim, Chris Hallacy, Aditya Ramesh, Gabriel Goh, Sandhini Agarwal, Girish Sastry, Amanda Askell, Pamela Mishkin, Jack Clark, et al. Learning transferable visual models from natural language supervision. In *ICML*, 2021.
- Aditya Ramesh, Mikhail Pavlov, Gabriel Goh, Scott Gray, Chelsea Voss, Alec Radford, Mark Chen, and Ilya Sutskever. Zero-shot text-to-image generation. In *ICML*, 2021.
- Aditya Ramesh, Prafulla Dhariwal, Alex Nichol, Casey Chu, and Mark Chen. Hierarchical text-conditional image generation with CLIP latents. *arXiv preprint arXiv:2204.06125*, 2022.
- Scott Reed, Zeynep Akata, Xinchun Yan, Lajanugen Logeswaran, Bernt Schiele, and Honglak Lee. Generative adversarial text to image synthesis. In *ICML*, 2016a.
- Scott E. Reed, Zeynep Akata, Santosh Mohan, Samuel Tenka, Bernt Schiele, and Honglak Lee. Learning what and where to draw. *NIPS*, 2016b.
- Jeremy Reizenstein, Roman Shapovalov, Philipp Henzler, Luca Sbordone, Patrick Labatut, and David Novotny. Common objects in 3D: Large-scale learning and evaluation of real-life 3D category reconstruction. In *ICCV*, 2021.
- Robin Rombach, Patrick Esser, and Björn Ommer. Network-to-network translation with conditional invertible neural networks. *NeurIPS*, 2020.
- Aditya Sanghi, Hang Chu, Joseph G Lambourne, Ye Wang, Chin-Yi Cheng, and Marco Fumero. CLIP-Forge: Towards zero-shot text-to-shape generation. In *CVPR*, 2022.
- Douglas M. Souza, Jônatas Wehrmann, and Duncan D. Ruiz. Efficient neural architecture for text-to-image synthesis. In *IJCNN*, 2020.
- David Stap, Maurits Bleeker, Sarah Ibrahim, and Maartje ter Hoeve. Conditional image generation and manipulation for user-specified content. *CVPRW*, 2020.
- Can Wang, Menglei Chai, Mingming He, Dongdong Chen, and Jing Liao. CLIP-NeRF: Text-and-image driven manipulation of neural radiance fields. In *CVPR*, 2022a.
- Hao Wang, Guosheng Lin, Steven Hoi, and Chunyan Miao. Cycle-consistent inverse GAN for text-to-image synthesis. *ACM MM*, 2021.
- Zihao Wang, Wei Liu, Qian He, Xinglong Wu, and Zili Yi. CLIP-GEN: Language-free training of a text-to-image generator with CLIP. In *arXiv preprint arXiv:2203.00386*, 2022b.
- Zixu Wang, Zhe Quan, Zhi-Jie Wang, Xinjian Hu, and Yangyang Chen. Text to image synthesis with bidirectional generative adversarial network. In *ICME*, 2020.
- Weihaio Xia, Yujiu Yang, Jing-Hao Xue, and Baoyuan Wu. TediGAN: Text-guided diverse face image generation and manipulation. In *CVPR*, 2021.
- Tao Xu, Pengchuan Zhang, Qiuyuan Huang, Han Zhang, Zhe Gan, Xiaolei Huang, and Xiaodong He. AttnGAN: Fine-grained text to image generation with attentional generative adversarial networks. In *CVPR*, 2018.
- Mingkuan Yuan and Yuxin Peng. Bridge-GAN: Interpretable representation learning for text-to-image synthesis. *IEEE TCSVT*, 2019.

-
- Han Zhang, Tao Xu, Hongsheng Li, Shaoting Zhang, Xiaogang Wang, Xiaolei Huang, and Dimitris N. Metaxas. StackGAN: Text to photo-realistic image synthesis with stacked generative adversarial networks. In *ICCV*, 2017.
- Han Zhang, Tao Xu, Hongsheng Li, Shaoting Zhang, Xiaogang Wang, Xiaolei Huang, and Dimitris N. Metaxas. StackGAN++: Realistic image synthesis with stacked generative adversarial networks. *IEEE TPAMI*, 2018.
- Yufan Zhou, Ruiyi Zhang, Changyou Chen, Chunyuan Li, Chris Tensmeyer, Tong Yu, Jiuxiang Gu, Jinhui Xu, and Tong Sun. LAFITE: Towards language-free training for text-to-image generation. In *CVPR*, 2022.
- Nikola Zubić and Pietro Liò. An effective loss function for generating 3D models from single 2D image without rendering. *arXiv preprint arXiv:2103.03390*, 2021.